Microfluidic chip for automated screening of carbon dioxide conditions for microalgal cell growth

Zhen Xu, Yingjun Wang, Yuncong Chen, Martin H. Spalding, and Liang Dong

Citation: Biomicrofluidics **11**, 064104 (2017);
View online: https://doi.org/10.1063/1.5012508
View Table of Contents: http://aip.scitation.org/toc/bmf/11/6
Published by the American Institute of Physics

Microfluidic chip for automated screening of carbon dioxide conditions for microalgal cell growth

Zhen Xu,[1] Yingjun Wang,[2] Yuncong Chen,[1] Martin H. Spalding,[2] and Liang Dong[1,a)]
[1]*Department of Electrical and Computer Engineering, Iowa State University, Ames, Iowa 50011, USA*
[2]*Department of Genetics, Development, and Cell Biology, Iowa State University, Ames, Iowa 50011, USA*

(Received 9 April 2017; accepted 6 November 2017; published online 22 November 2017)

This paper reports on a microfluidic device capable of screening carbon dioxide (CO_2) conditions for microalgal cell growth. The device mainly consists of a microfluidic cell culture (MCC) unit, a gas concentration gradient generator (CGG), and an in-line cell growth optical measurement unit. The MCC unit is structured with multiple aqueous-filled cell culture channels at the top layer, multiple CO_2 flow channels at the bottom layer, and a commercial hydrophobic gas semipermeable membrane sandwiched between the two channel layers. The CGG unit provides different CO_2 concentrations to support photosynthesis of microalgae in the culture channels. The integration of the commercial gas semipermeable membrane into the cell culture device allows rapid mass transport and uniform distribution of CO_2 inside the culture medium without using conventional agitation-assisted convection methods, because the diffusion of CO_2 from the gas flow channels to the culture channels is fast over a small length scale. In addition, automated in-line monitoring of microalgal cell growth is realized via the optical measurement unit that is able to detect changes in the light intensity transmitted through the cell culture in the culture channels. The microfluidic device also allows a simple grayscale analysis method to quantify the cell growth. The utility of the system is validated by growing *Chlamydomonas reinhardtii* cells under different low or very-low CO_2 levels below the nominal ambient CO_2 concentration. *Published by AIP Publishing.* https://doi.org/10.1063/1.5012508

INTRODUCTION

Microalgae are microorganisms that can rapidly grow by using inexpensive renewable resources, such as light, CO_2, water, and certain inorganic salts, to produce biomass and oil production.[1] Compared with higher plants, microalgae have higher rates of biomass and oil production than traditional crops, due to their simple cellular structure.[2] Presently, microalgae cultivation is performed in flasks, dishes, and plates[3] for laboratory research and open raceway ponds[4] and tubular, flat, and vertical photobioreactors in various pilot plants.[5–9] These systems allow small to large-scale algae cultivation for studying influences of combinatorial conditions (e.g., light,[10,11] temperature,[12] CO_2,[13] pH,[14] and nutrients[15–17]) on photosynthesis of microalgal cells. To maximize microalgal biomass and lipid production, it is critical to select and develop more efficient microalgal strains and find optimal cultivation conditions through advanced genetic and biochemical approaches and assay technologies.[18] However, traditional cultivation systems are often not suitable for rapid screening of numerous microalgal strains and their optimal growth conditions to isolate superior strains. In addition to their relatively large footprint areas, high material consumptions, and slow response times, it is also challenging to simultaneously create multiple sets of different environmental conditions with high accuracy and flexibility.

a)Author to whom correspondence should be addressed: ldong@iastate.edu

Microfluidics-based biotechnologies have been extensively developed to enable system miniaturization, automation, and parallelization of biochemical processes,[19] as well as high-throughput culture, manipulation, and detection of cells and microorganisms.[20–26] Several microfluidic devices have been reported for on-chip cultivation, analysis, and transformation of microalgal cells under various growth conditions.[27–42] For example, toxicity screening using marine microalgal cultures in a microfluidic device was reported.[39] Microfluidic photobioreactors were also realized to study the impact of light conditions on microalgal cell growth and oil production.[40,41] In addition, microfluidic droplets were utilized to study growth kinetics of microalgae.[42]

The current atmospheric CO_2 level (approximately 400 ppm or so-called low CO_2) is one of the major limiting factors for optimal photosynthesis and biomass accumulation in many plant and algal species.[43] Microalgal cells grown under atmospheric CO_2 level (with or without active aeration) can draw more than 80% CO_2 from the medium through photosynthesis, reducing the actual CO_2 level into the range of near deplete (so-called very-low CO_2 concentration) far below the nominal ambient CO_2 concentration.[13,44] Multiple acclimation states have been demonstrated in the model green alga *Chlamydomonas* in response to these different low- or very low-CO_2 conditions, which are driven by different inorganic carbon uptake modes and regulatory mechanism.[45] One advantage of microfluidics-based bioreactors is their small volume in which different environmental conditions can be rapidly and precisely controlled. This is especially useful to control CO_2 status for microalgal cell cultures (MCCs) because fast equilibrium between the gas and liquid phases can be achieved. To our knowledge, there are no reports on the development of microfluidic devices to study the microalgal cell growth under various CO_2 conditions. In-line monitoring of microalgae growth has also rarely been achieved in existing microfluidic algae bioreactors.

In this paper, we report on a new microfluidic device for parallel execution of microalgal cell culture experiments and in-line monitoring of cell growth under different low- or very-low CO_2 conditions. Spatial CO_2 concentrations inside cell culture channels can be precisely obtained and uniformly distributed within only a few minutes, due to the unique integration of a hydrophobic gas semipermeable membrane into the device. Specifically, the device consists of a microalgal cell culture (MCC) unit and a gas concentration gradient generation (CGG) unit [Fig. 1(a)]. The MCC unit is structured with multiple aqueous-filled cell culture channels at the top layer, multiple CO_2 flow channels at the bottom layer, and a hydrophobic gas semipermeable membrane sandwiched between these two layers [Figs. 1(b) and 1(c)]. The CGG unit can generate a series of different gas concentrations to provide CO_2 supplies for growing cells in the culture channels. The gas inlets of the MCC unit are located at the back of the unit [Fig. 1(a)]. The MCC and CGG units are connected using microfluidic tubing.

DEVICE DESIGN

The sandwiched hydrophobic gas semipermeable membrane holds the aqueous culture medium in the upper cell culture channels, while allowing CO_2 to diffuse from the gas flow channels into the growth medium through the embedded nanopores of this membrane. Here, the mass transport of CO_2 into the medium is fast, as it relies on direct diffusion over a small length scale, rather than on using agitation-assisted convection methods (e.g., shaking, rotating, and bubbling) of traditional cultivation systems. Because the whole upper culture channel is exposed to the CO_2 flowing in the gas channel, the diffusion of CO_2 will lead to uniform gas distribution within the aqueous-filled culture channel. In addition, the use of the nanoporous semipermeable membrane avoids large-area contact of the medium with the CO_2 flow that otherwise will cause a notorious evaporation problem often occurring with air-open microfluidic devices. Nevertheless, minor evaporation still happens at the nanopores in the membrane. To compensate for possible medium losses, two miniature reservoirs are emplaced at the inlet and outlet of each culture channel and loaded with minimal medium (Fig. 1). Here, the minimal medium does not have any organic carbon acetate so microalgae can only use CO_2 as a carbon

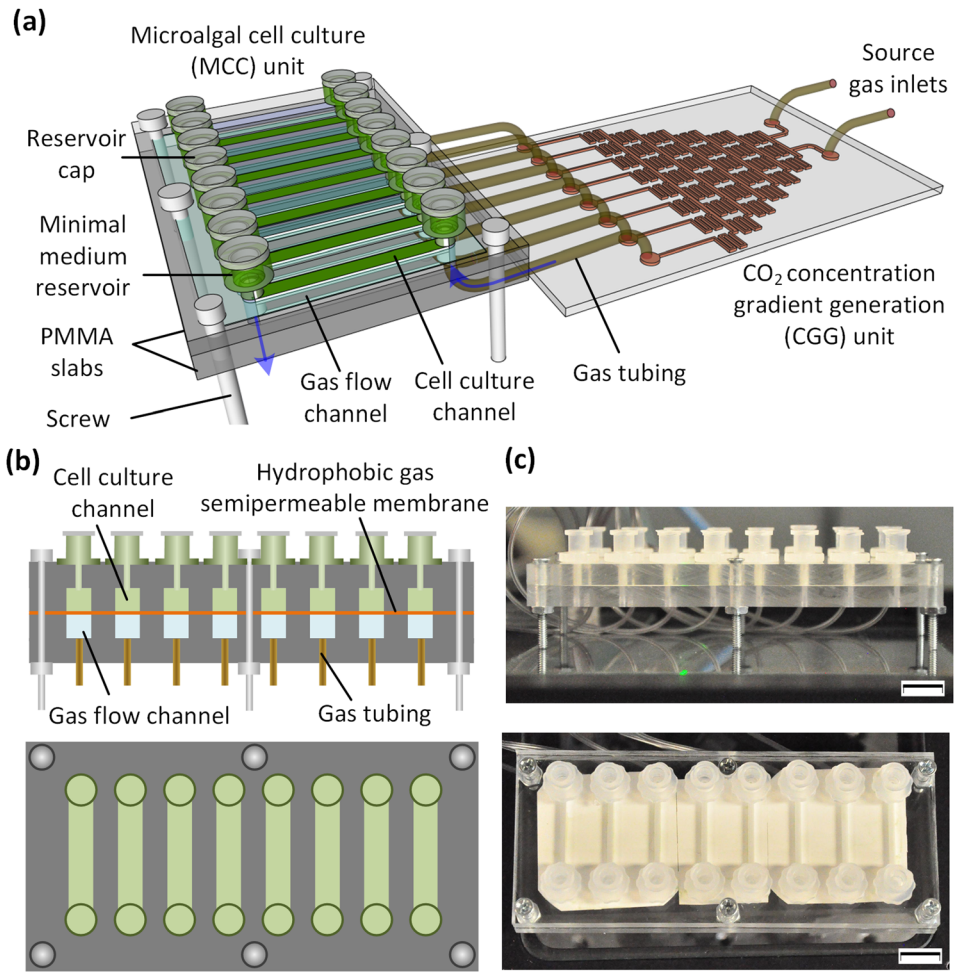

FIG. 1. (a) Schematic of a microfluidic device with a MCC unit and a CGG unit for growing microalgal cells under different CO_2 conditions. (b) and (c) Side view (upper panel) and top view (lower panel) of the MCC unit [(b) schematic representations and (c) photos of a fabricated device]. The scale bars in (c) represent 5 mm.

source. The level of medium surface in the reservoirs is set above the culture channel. This allows automatic refilling of the culture channel when the medium loss occurs.

Dynamic process of CO_2 diffusion from the gas flow channel to the cell culture channel was studied using a finite element analysis (FEA) based software COMSOL. The CO_2 gas diffuses through the membrane and further into the culture channel [Fig. 2(a)]. The diffusion process was modelled using the mass transport equation described below[46]

$$(\partial c/\partial t) + \nabla \cdot (-D\nabla c) + d = 0, \tag{1}$$

where c, D, and d represent the concentration, diffusivity, and constant consumption rate of CO_2, respectively. The growth medium in the culture channel was in a static state. The diffusion coefficient of CO_2 was set $D = 1.44 \times 10^{-5}$ m^2/s in the nanoporous membrane, 1.92×10^{-9} m^2/s in the aqueous culture medium,[47] and 3.16×10^{-13} m^2/s in the channel material, i.e., poly(methyl methacrylate) or PMMA[48] (which is negligibly small compared with those in the former two materials). The permeability of CO2 in PMMA was set 5×10^{-11} cm^3 (STP)·cm/cm^2·s·cm Hg.[49] The walls of the PMMA channel were treated as no-slip walls. For a normalization purpose, a constant CO_2 concentration $c = 1.0\,mol/m^3$ was used. It is noteworthy that the CO_2 consumption rate of microalgal cells is significantly affected by cell photosynthesis, inducible CO_2 concentrating mechanism, and other factors.[50–53] For example, microalgal cells can

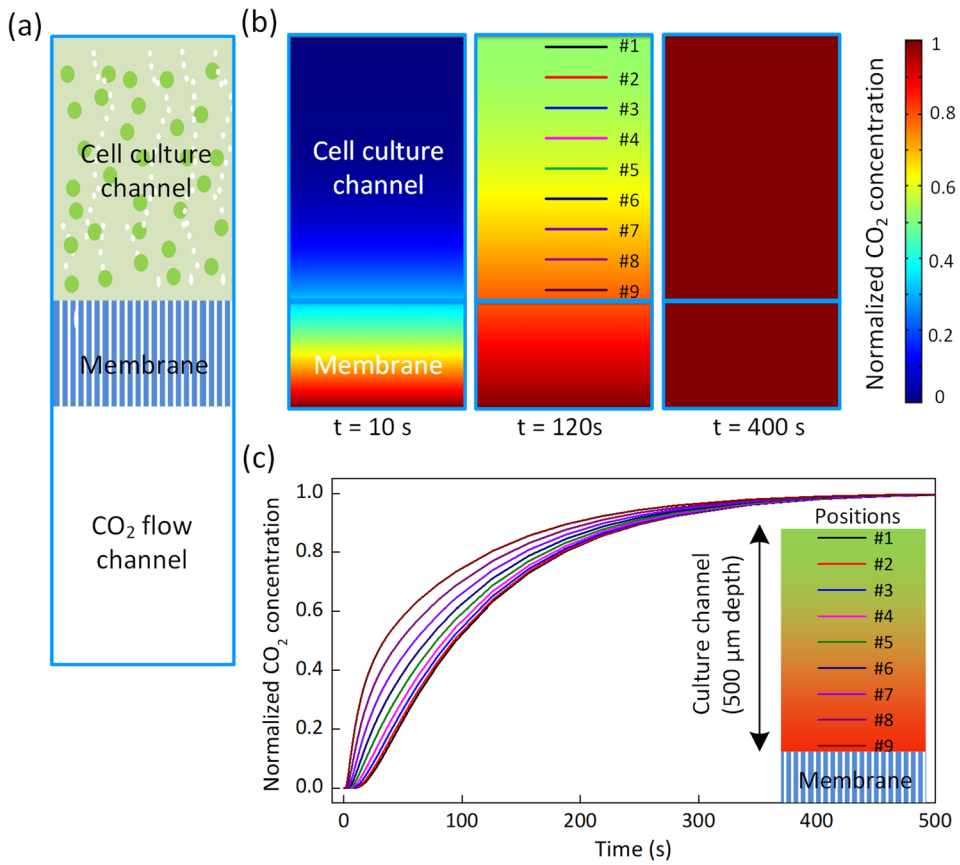

FIG. 2. (a) Schematic side view of a set of cell culture, gas flow channel, and hydrophobic gas semipermeable membrane. (b) Simulated time-lapse images showing the diffusion of CO_2 through the membrane into an aqueous-filled culture channel. The CO_2 channel is not shown here. The color bar on the right indicates the normalized CO_2 concentration. (c) Simulated normalized CO_2 concentration as a function of time at nine different positions in the vertical direction of the culture channel. These positions are also labeled in the second panel of (b).

actively and dynamically accumulate CO_2 at the site of ribulose-1,5-bisphosphate carboxylase-oxygenase (RuBisCO). Because of the complexity of dynamic CO_2 concentrating process inside the cell,[13] it is not easy to obtain and apply a time-varying CO_2 consumption rate in Eq. (1). Here, to illustrate the diffusion process only, the CO_2 consumption rate was set constant at $d = 5.70 \times 10^{-10}$ mol/(m^3·s) based on the information given in Ref. 54. Figure 2(b) shows the simulated time-lapse CO_2 distribution in the 500 μm-deep aqueous-filled culture channel above the gas semipermeable hydrophobic membrane (thickness: 200 μm and mean pore size: 220 nm). In addition, nine observation positions were set in the vertical direction of the culture channel to exam the time required for CO_2 to reach diffusion equilibrium at different locations in the culture channel. These positions were equally spaced across the height of the culture channel. Figure 2(c) shows that CO_2 in the culture medium closer to the membrane reaches a stable level slightly earlier than that farther from the membrane. After only about 400 s, the whole culture channel has a uniformly distributed CO_2 environment.

Figure 3(a) shows the gas CGG unit able to produce eight different CO_2 concentrations. This unit was formed with two gas inlets, eight outlets, and a series of serpentine channels between the inlets and outlets.[55] All the channels in this unit were set 200 μm wide and 50 μm deep. As two source CO_2 streams (50 ppm and 280 ppm) were introduced into the device, they travelled down, repeatedly split, combined with neighboring streams, and mixed by diffusion in the serpentine channels [Fig. 3(b)]. Here, because this work was focused on studying microalgal cell growth under low or very-low CO_2 levels below the nominal ambient CO_2 concentration, 50 ppm and 280 ppm were selected as two input concentrations of the CGG unit to create eight

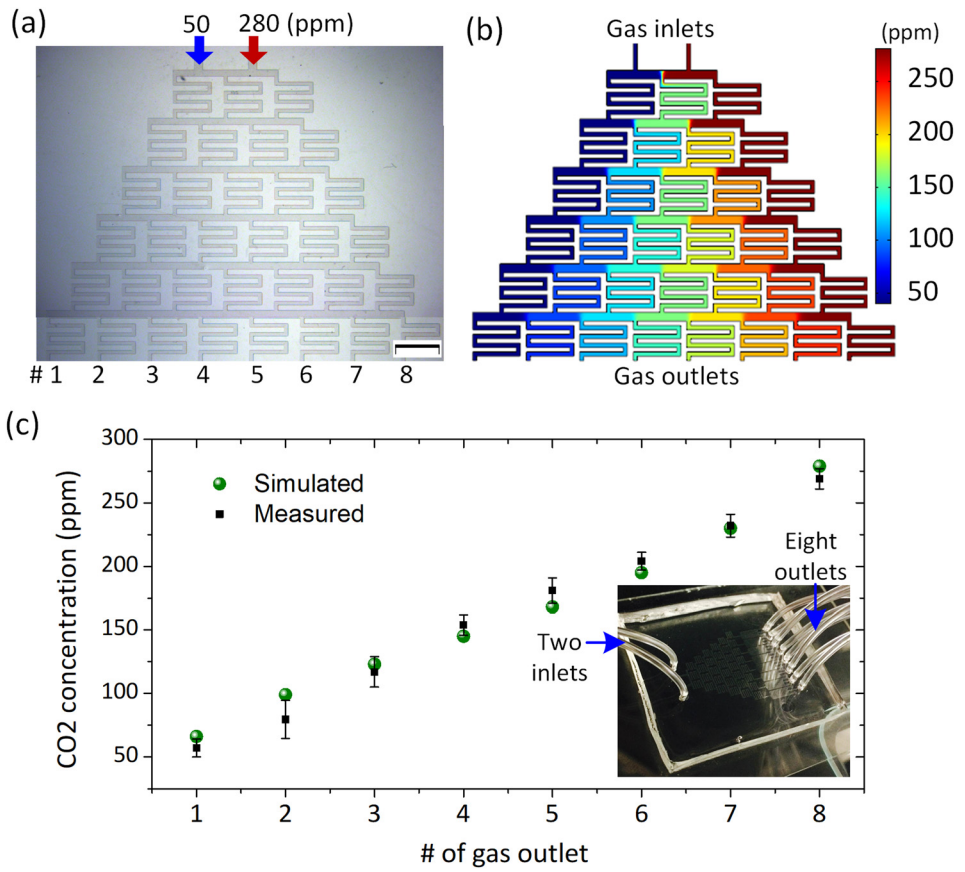

FIG. 3. (a) Microscopic image for the channel network of the gas CGG unit. (b) Simulated steady-state CO_2 distribution. The scale bars represent 2 mm. (c) Measured and simulated CO_2 levels at the outputs of the unit. The measurements were performed using a CO_2 meter (Qubit Systems: Kingston, ON, Canada). The inset shows the fabricated CGG device. The result was obtained over four independent experiments with four devices.

different CO_2 levels in a range set by these two source concentrations. In order to achieve uniform mixing of the two source gases, six mixing layers were utilized in the CGG unit, and the total channel length from one inlet to one outlet was set 28 mm [Figs. 3(a) and 3(b)]. This design resulted in a stable discrete gradient of CO_2 levels generated at the outlets of the device. The measured CO_2 concentrations agreed with the simulated result [Fig. 3(c)].

The cell culture and gas flow channels of the MCC unit were formed with two PMMA plates (thickness: 0.25 in.; Plexiglas: Alsip, IL) using a milling machine (CNC Masters, Irwindale, CA). All the channels had dimensions of 0.5 mm (depth) × 1 mm (width) × 10 mm (length) and were manually aligned. The hydrophobic semipermeable membrane (thickness: 200 μm and mean pore size: 220 nm; Sterlitech: Kent, WA) was sandwiched by the PMMA plates with six cap screws (M4 × 0.7; Thorlabs: Newton, NJ). After that, 16 polypropylene reservoirs (EW-45508-16; Cole-Parmer: Vernon Hills, IL) with 100 μl loading volume were glued at the ends of the culture channels. The CGG unit was made of poly(dimethyl siloxane) or PDMS using conventional soft lithography. Finally, microfluidic tubing (Microbore PTFE tubing; 0.012″ ID × 0.030″ OD; Cole-Parmer, Vernon Hills, IL) was used to direct the gas flows from the outlets of the CGG to the MCC unit.

EXPERIMENTAL

To realize in-line monitoring of microalgal cell growth, an optical detection system [Fig. 4(b)] was built to measure the transmitted light intensity (TLI) varying with growing cells in the culture channels. The detection system mainly consists of a 532-nm wavelength laser

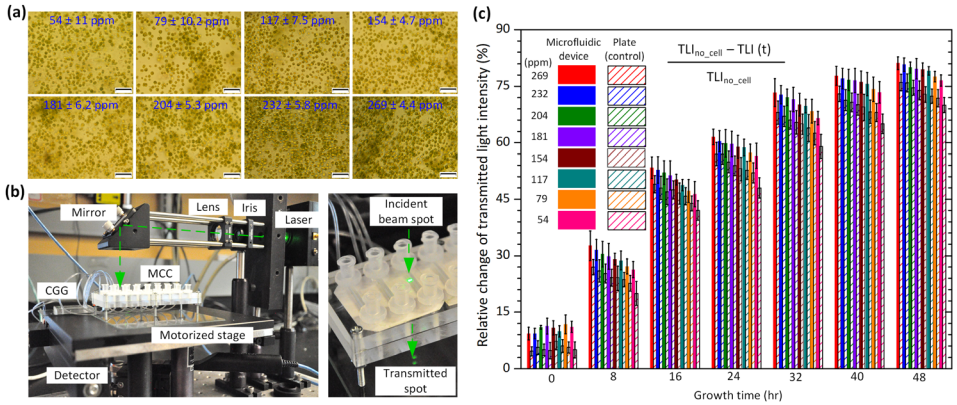

FIG. 4. (a) Microscopic images of *C. reinhardtii* strain CC620 grown in the eight channels of the MCC unit with different CO_2 concentration levels labelled. The scale bars represent 40 μm. (b) TLI measurement setup (left). (c) Relative change in TLI as a function of CO_2 concentration over a 48-h period for cultivation of cells (*C. reinhardtii* strain CC620) in both the microfluidic device and the plates. The result was obtained over four independent experiments with four devices.

(DJ532-10; Thorlabs: Newton, NJ), a photodetector (model 1918; Newport, Irvine, CA), and a programmable motorized stage (ASI-FW1000: Applied Scientific Instrumentation, Eugene, OR). The 532-nm wavelength was chosen to minimize direct light absorption by microalgal cells.[56] The motorized stage allowed precise positioning of each culture channel under the beam spot (diameter: 0.8 mm) for the TLI measurement.

A common laboratory microalgal strain of *Chlamydomonas reinhardtii* (*C. reinhardtii*, CC620) was used as a model cell to validate the developed device. The strain was obtained from the Chlamydomonas Resource Centre and maintained on agar plates with Tris-acetate-phosphate (TAP) nutrient in a Plexiglass chamber at room temperature under light.[57] Liquid cultures were grown in flasks on an incubated orbital shaker at 125 rpm. In both the plate and liquid cultures, a 5% CO_2 flow (in air vol/vol) was maintained in the incubator.

To perform on-chip cell culture, all the device components were sterilized by filling with pure ethanol and letting them sit for 1 h, followed by flushing the components with deionized water for 5 min and then minimal medium without carbon (consisting of 143 mg/l K_2HPO_4, 73 mg/l KH_2PO_4, 400 mg/l NH_4NO_3, 100 mg/l $MgSO_4.7\ H_2O$, 50 mg/l $CaCl_2{\cdot}2H_20$, 1 ml/l trace elements stock,[58] and 10 ml/l 2.0 M Mops titrated with Tris base to pH 7.1) for another 5 min. 1 ml of the strain CC620 (pre-incubated in flasks as described above) was used to mix with TAP medium in a 10-ml centrifuge tube (Corning: Corning, NY). The cells were then separated from TAP medium by centrifuging (Champion F-33V: Ample Scientific, Norcross, GA) at 2000 rpm for 5 min and mixed with 10 ml minimal medium.[59]

After the cells were loaded into the culture channels using a pipette, the miniature polypropylene reservoirs were filled with the minimal medium and sealed with homemade PDMS plugs. The cells were grown under a 9-W fluorescent lamp placed 30 cm above the culture channels. Eight CO_2 concentrations were realized at the outputs of the CGG unit [Fig. 3(c)] by infusing 50 ppm and 280 ppm source CO_2 flows into the unit through two gas flow controllers (EW-32660: Cole-Parmer, Vernon Hills, IL).

RESULTS AND DISCUSSION

Under the generated CO_2 environments, the strain CC620 was grown in the culture channels for 48 h. Figure 4(a) shows that the cell density increased differently at 48 h, depending on the exposed CO_2 levels. To quantify the CO_2 impact, the cell growth under different CO_2 conditions was monitored using the TLI measurement setup once every 8 h. Ten different areas were tested for each culture channel. Figure 4(c) shows the relative change in TLI compared with the initial TLI value (obtained prior to cell loading with only the minimal medium in the channel). The calculation method is displayed in Fig. 4(c), where the variables of TLI_{no_cell} and

TLI(t) represent the initial TLI value and the value at time t, respectively. In each channel, the cell density increased with time t owing to cell growth and division, causing to reduce the absolute value of TLI. Therefore, there appears to be an increase in the relative change in TLI over a 48-h period under all the different CO_2 conditions [Fig. 4(c)]. In addition, the relative change in TLI increased with CO_2 concentration, indicating that the higher CO_2 concentrations (in the tested range from 54 ppm to 269 ppm) promoted the cell growth. Specifically, at 48 h, the relative TLI change was shown to increase from 70% at 54 ppm CO_2 concentration to 77% at 269 ppm [Fig. 4(c)].

In the control experiment, a 5 ml cell suspension solution (pre-incubated using the above-mentioned method) with the minimal medium were loaded in a sterile Petri dish (3.5 cm diameter and 1 cm depth; SIAL0165: Sigma-Aldrich, St. Louis, MO) emplaced inside an incubator. Eight CO_2 concentrations were provided by mixing 5% CO_2 (in air vol/vol) with dry CO_2-free air with the help of two flow controllers. The obtained CO_2 levels were the same as those used in the microfluidic culture experiment. The TLI measurement was performed outside the incubator at an 8-h interval. It should be noted that the relative change in TLI from the control experiment exhibited an almost parallel rise over all the CO_2 levels compared with those from the on-chip growth experiment. This may be due to the larger quantity of cells initially loaded in the Petri dishes than that loaded into the microfluidic culture channels. Nevertheless, the tendencies to increase the relative change in TLI with increasing CO_2 level agreed well between the two methods. This result indicates that our device is suitable for cultivation of microalgal cells.

In addition to the TLI measurement, the microfluidic device also allowed a simple grayscale analysis method to quantify cell growth in the channels. Such redundancy will be helpful for those users who may not be able to access the optical TLI measurement setup. As the cells grew, the color of culture channel became darker. A digital camera (DFC310 FX; Leica: Wetzlar, Germany) was used to regularly take photos of the culture channels. The grayscale value (GSV; 0 = totally dark and 255 = totally bright) of the channel image was extracted by Image J (an open source image processing and analysis freeware). The change in GSV at time t was compared with its initial value at t = 0 (right after cell loading) and then further normalized by the initial GSV (see the calculation method displayed in Fig. 5). As shown in Fig. 5, under a generated CO_2 concentration, the GSV of the channel image gradually decreased in a 48-h span, implying the increase in cell density. The higher the CO_2 concentration, the more the relative change in GSV obtained. At 48 h, the maximum relative reduction in GSV (53%)

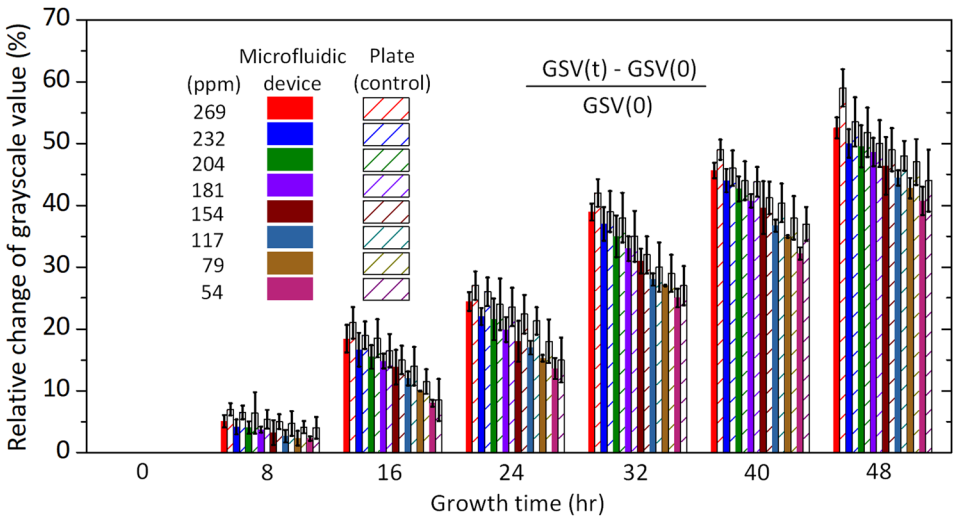

FIG. 5. Relative change in GSV of the images of cell culture channels containing *C. reinhardtii* strain CC620 growing under different CO_2 levels over a 48-h period. At time t = 0, the relative changes in GSV for all the culture channels are zero. The result was obtained over four independent experiments with four devices.

occurred at 269 ppm and the minimum (41%) at 54 ppm. The results were also validated by the control experiment previously described, except for performing the GSV measurement in this case. Due to the different nature of the TLI and GSV methods, the obtained relative changes in TLI [Fig. 4(c)] and GSV (Fig. 5) are not necessary to be the same.

This work was focused on proof-of-concept for using the microfluidic device to cultivate microalgal cells under different low- or very low-CO_2 conditions. It would be readily possible to enhance the processing ability of the device to conduct parallel microalgal cell culture experiments, by simply varying the source CO_2 levels and increasing the numbers of CO_2 flow and cell culture channels. In order to study microalgal cell growth under high CO_2 conditions, the presented CGG unit can be interfaced with two appropriate CO_2 source gases at its two inlets. It is also our interest to integrate this device with other detection methods (e.g., fluorescence) to study the lipid content of microalgal species and strains as a function of CO_2 concentration. This will help us to better understand cellular phenomena and mechanisms (e.g., lipid metabolism, CO_2 accumulating, and environmental adaptability) controlling growth and oil content and to find high oil producing strains. In addition, we note that although the CO_2 concentrations in the gas flow channels were measured using the commercial CO_2 sensor mentioned above, it is challenging to directly measure the dissolved CO_2 concentrations in the liquid growth media because the presently commercial CO_2 sensors are all too big to fit in the small culture channels. It should be noted that based on Henry's Law,[60] the dissolved CO_2 concentration in the liquid culture channel is actually linear with the CO_2 concentration in the gas flow channel, as the environmental temperature and air pressure are constant over time. One of our future works is to develop dissolved CO_2 sensors (or pH sensors[61]) that are small enough to be embedded into the culture channels of the presented microfluidic system. In addition, it would be useful to integrate controlled chemical delivery[62,63] and temperature control elements[64] to facilitate studying the influence of various biotic and abiotic stresses on different microalgal cell species and strains. Finally, to understand cellular activities under low or very-low CO_2 conditions, some functional tests at the cellular level with these low CO_2 concentrations will be performed on the chip.

CONCLUSIONS

We have demonstrated a microfluidic device to cultivate microalgal cells under different low or very-low CO_2 concentrations and perform in-line measurement of cell growth rate, which is difficult to be done in traditional large-batch growth. The integration of the gas semi-permeable hydrophobic membrane into the cell culture device allowed rapid mass transportation and uniform distribution of CO_2 in the culture medium within only several minutes. In addition, useful methodological redundancy (i.e., both TLI and GSV measurements) for monitoring of cell growth have been developed, which will increase the adoptability of this microfluidic device by a wide range of users.

ACKNOWLEDGMENTS

This work was supported in part by the Plant Sciences Institute through the Faculty Scholar Program and the Crop Bioengineering Consortium through the CBC Seed Grant Program, both at Iowa State University, and in part by the U.S. National Science Foundation under Grant Nos. DBI-1353819 and IOS-1650182. The authors thank Dr. Dan Stessman for providing microalgal cells and culture media.

[1]S. A. Scott, M. P. Davey, J. S. Dennis, I. Horst, C. J. Howe, D. J. Lea-Smith, and A. G. Smith, Curr. Opin. Biotechnol. **21**(3), 277–286 (2010).
[2]M. Packer, Energy Policy **37**(9), 3428–3437 (2009).
[3]A. Saeed and M. Iqbal, World J. Microbiol. Biotechnol. **22**(8), 775–782 (2006).
[4]O. Jorquera, A. Kiperstok, E. A. Sales, M. Embiruçu, and M. L. Ghirardi, Bioresour. Technol. **101**(4), 1406–1413 (2010).
[5]C.-Y. Chen, K.-L. Yeh, R. Aisyah, D.-J. Lee, and J.-S. Chang, Bioresour. Technol. **102**(1), 71–81 (2011).
[6]D. O. Hall, F. Acién Fernández, E. C. Guerrero, K. K. Rao, and E. M. Grima, Biotechnol. Bioeng. **82**(1), 62–73 (2003).
[7]J. C. Ogbonna, T. Soejima, and H. Tanaka, J. Biotechnol. **70**(1), 289–297 (1999).
[8]J. Pruvost, L. Pottier, and J. Legrand, Chem. Eng. Sci. **61**(14), 4476–4489 (2006).

[9]C. Ugwu, H. Aoyagi, and H. Uchiyama, Bioresour. Technol. **99**(10), 4021–4028 (2008).
[10]E. Collini, C. Y. Wong, K. E. Wilk, P. M. Curmi, P. Brumer, and G. D. Scholes, Nature **463**(7281), 644–647 (2010).
[11]W. Dunstan, J. Exp. Mar. Biol. Ecol. **13**(3), 181–187 (1973).
[12]I. R. Davison, J. Phycol. **27**(1), 2–8 (1991).
[13]P. Vance and M. H. Spalding, Can. J. Bot. **83**(7), 796–809 (2005).
[14]Y. Azov, Appl. Environ. Microbiol. **43**(6), 1300–1306 (1982).
[15]W. A. Kratz and J. Myers, Am. J. Bot. **42**, 282–287 (1955).
[16]M. F. Pedersen and J. Borum, Mar. Ecol. Prog. Ser. **142**, 261–272 (1996).
[17]J. Yang, M. Xu, X. Zhang, Q. Hu, M. Sommerfeld, and Y. Chen, Bioresour. Technol. **102**(1), 159–165 (2011).
[18]R. Radakovits, R. E. Jinkerson, A. Darzins, and M. C. Posewitz, Eukaryotic Cell **9**(4), 486–501 (2010).
[19]D. Mark, S. Haeberle, G. Roth, F. von Stetten, and R. Zengerle, Chem. Soc. Rev. **39**(3), 1153–1182 (2010).
[20]G. B. Salieb-Beugelaar, G. Simone, A. Arora, A. Philippi, and A. Manz, Anal. Chem. **82**(12), 4848–4864 (2010).
[21]H. Yang, X. Qiao, M. K. Bhattacharyya, and L. Dong, Biomicrofluidics **5**, 044103 (2011).
[22]R. A. Erickson and R. Jimenez, Lab Chip **13**(5), 2893–2901 (2013).
[23]H. Jiang, Z. Xu, M. R. Aluru, and L. Dong, Lab Chip **14**(7), 1281–1293 (2014).
[24]P. Liu, R. J. Martin, and L. Dong, Lab Chip **13**(4), 650–661 (2013).
[25]Z. Xu, H. Jiang, B. B. Sahu, S. Kambakam, P. Singh, X. Wang, Q. Wang, M. K. Bhattacharyya, and L. Dong, Biomicrofluidics **10**(5), 034108 (2016).
[26]P. Liu, D. Mao, R. J. Martin, and L. Dong, Lab Chip **12**(18), 3458–3466 (2012).
[27]A. Han, H. Hou, L. Li, H. S. Kim, and P. de Figueiredo, Trends Biotechnol. **31**(4), 225–232 (2013).
[28]R. E. Holcomb, L. J. Mason, K. F. Reardon, D. M. Cropek, and C. S. Henry, Anal. Bioanal. Chem. **400**(1), 245–253 (2011).
[29]D.-H. Lee, C. Y. Bae, J.-I. Han, and J.-K. Park, Anal. Chem. **85**(18), 8749–8756 (2013).
[30]J. Pan, A. L. Stephenson, E. Kazamia, W. T. Huck, J. S. Dennis, A. G. Smith, and C. Abell, Integr. Biol. **3**(10), 1043–1051 (2011).
[31]A. Schaap, Y. Bellouard, and T. Rohrlack, Biomed. Opt. Expres. **2**(3), 658–664 (2011).
[32]A. Schaap, T. Rohrlack, and Y. Bellouard, Lab Chip **12**(8), 1527–1532 (2012).
[33]D. R. Link, E. Grasland-Mongrain, A. Duri, F. Sarrazin, Z. Cheng, G. Cristobal, M. Marquez, and D. A. Weitz, Angew. Chem., Int. Ed. **45**(16), 2556–2560 (2006).
[34]S. Bae, C. W. Kim, J. S. Choi, J. W. Yang, and T. S. Seo, Anal. Bioanal. Chem. **405**(29), 9365–9374 (2013).
[35]R. Best, S. Abalde-Cela, C. Abell, and A. G. Smith, Curr. Biotechnol. **5**(2), 109–117 (2016).
[36]I. B. Tahirbegi, J. Ehgartner, P. Sulzer, S. Zieger, A. Kasjanow, M. Paradiso, and T. Mayr, Biosens. Bioelectron. **88**, 188–195 (2017).
[37]H. S. Kwak, J. Y. H. Kim, S. C. Na, N. L. Jeon, and S. J. Sim, Analyst **141**(4), 1218–1225 (2016).
[38]H. S. Kim, A. R. Guzman, H. R. Thapa, T. P. Devarenne, and A. Han, Biotechnol. Bioeng. **113**(8), 1691–1701 (2016).
[39]G. Zheng, Y. Wang, Z. Wang, W. Zhong, H. Wang, and Y. Li, Mar. Pollut. Bull. **72**(1), 231–243 (2013).
[40]M. Chen, T. Mertiri, T. Holland, and A. S. Basu, Lab Chip **12**(20), 3870–3874 (2012).
[41]H. S. Kim, T. L. Weiss, H. R. Thapa, T. P. Devarenne, and A. Han, Lab Chip **14**(8), 1415–1425 (2014).
[42]A. Dewan, J. Kim, R. H. McLean, S. A. Vanapalli, and M. N. Karim, Biotechnol. Bioeng. **109**(12), 2987–2996 (2012).
[43]Y. Wang, D. J. Stessman, and M. H. Spalding, Plant J. **82**(3), 429–448 (2015).
[44]T. Yamano, K. Miura, and H. Fukuzawa, Plant Physiol. **147**(1), 340–354 (2008).
[45]Y. Wang and M. H. Spalding, Proc. Natl. Acad. Sci. U.S.A. **103**(26), 10110–10115 (2006).
[46]J. S. Rowlinson, Chem. Br. **20**(11), 1027–1027 (1984).
[47]T. R. Marrero and E. A. Mason, J. Phys. Chem. Ref. Data **1**(1), 3–118 (1972).
[48]H. Eslami *et al.*, J. Chem. Phys. **139**(12), 124902 (2013).
[49]M. Schutze, B. Isecke, and R. Bender, *Corrosion Protection against Carbon Dioxide* (Wiley-VCH Verlag, Weinheim, Germany, 2011), p. 130.
[50]Y. Wang and M. H. Spalding, Plant Physiol. **166**(4), 2040–2050 (2014).
[51]M. R. Badger and M. H. Spalding, *Photosynthesis* (Springer, 2000), pp. 369–397.
[52]G. Bozzo and B. Colman, Plant, Cell Environ. **23**(10), 1137–1144 (2000).
[53]M. R. Badger, A. Kaplan, and J. A. Berry, Plant Physiol. **66**(3), 407–413 (1980).
[54]J. L. Gosse, M. S. Chinn, A. M. Grunden, O. I. Bernal, J. S. Jenkins, C. Yeager, S. Kosourov, M. Seibert, and M. C. Flickinger, J. Ind. Microbiol. Biotechnol. **39**(9), 1269–1278 (2012).
[55]S. K. Dertinger, D. T. Chiu, N. L. Jeon, and G. M. Whitesides, Anal. Chem. **73**(6), 1240–1246 (2001).
[56]Y. Y. Huang, C. M. Beal, W. W. Cai, R. S. Ruoff, and E. M. Terentjev, Biotechnol. Bioeng. **105**(5), 889–898 (2010).
[57]D. S. Gorman and R. Levine, Proc. Natl. Acad. Sci. U.S.A. **54**(6), 1665–1669 (1965).
[58]S. Surzycki, Methods Enzymol. **23**, 67–73 (1971).
[59]A. M. Geraghty, J. C. Anderson, and M. H. Spalding, Plant Physiol. **93**(1), 116–121 (1990).
[60]W. Gerrard, "Henry's Law and Raoult's Law," in *Solubility of Gases and Liquids* (Springer, 1976), pp. 29–54.
[61]D. Mao, P. Liu, and L. Dong, J. Polym. Sci. B: Phys. **49**, 1645–1650 (2011).
[62]H. Yang, W. Hong, and L. Dong, Appl. Phys. Lett. **100**, 153510 (2012).
[63]H. Yang and L. Dong, Langmuir **26**, 1539–1543 (2010).
[64]H. W. Jiang, Y. Jiao, M. R. Aluru, and L. Dong, J. Nanosci. Nanotechnol. **12**, 6333–6639 (2012).